



HAL
open science

A GIS-based atmospheric dispersion model

N. Bozon, C. Sinfort, B. Mohammadi

► **To cite this version:**

N. Bozon, C. Sinfort, B. Mohammadi. A GIS-based atmospheric dispersion model. STIC & Environnement, Jun 2009, Calais, France. 17 p. hal-00468863

HAL Id: hal-00468863

<https://hal.science/hal-00468863>

Submitted on 31 Mar 2010

HAL is a multi-disciplinary open access archive for the deposit and dissemination of scientific research documents, whether they are published or not. The documents may come from teaching and research institutions in France or abroad, or from public or private research centers.

L'archive ouverte pluridisciplinaire **HAL**, est destinée au dépôt et à la diffusion de documents scientifiques de niveau recherche, publiés ou non, émanant des établissements d'enseignement et de recherche français ou étrangers, des laboratoires publics ou privés.

A GIS-based atmospheric dispersion model

Nicolas Bozon* — **Carole Sinfort**** — **Bijan Mohammadi*****

* *Cemagref - UMR ITAP*
BP 5095
F-Montpellier
nicolas.bozon@gmail.com

** *Montpellier SupAgro - UMR ITAP*
2 pl. Viala
F-34060 Montpellier
sinfort@supagro.inra.fr

*** *Université Montpellier 2 - UMR5149*
Mathematical Modelling Institute
F-34095 Montpellier
bijan.mohammadi@universite-montpellier2.eu

ABSTRACT. Atmospheric pollution due to the use of agricultural pesticide is a major concern today, regarding both public health, sustainable agriculture and ecosystems quality monitoring. This work aims to model pesticide atmospheric dispersion and to propose an useful air pollution prediction tool, using fluid mechanics equations and open-source GIS programming capabilities. This work focuses on pesticide spray drift modelling for viticulture applications from the plot to the watershed scales. Our goal is to provide a GIS based atmospheric transport simulation platform at very low calculation cost using solution space reduction and reduced order modelling. This is necessary to make affordable simulation and very helpful to quickly perform georeferenced pollution predictions, which can then be used as a basis for risk analysis. The coupling of fluid mechanic equations with GIS is first described, regarding the enhancement of the mathematical model according to GIS parameters like topography and scale variations. Indeed, ground variations are implemented in the model using digital elevation model (DEM). The use of DEM is an asset to replace former Cartesian outputs by georeferenced raster pesticide cloud and also, it allows to use the model on any area. Furthermore, the implementation of topography in the spatialized Gaussian plume model allows scale changes. The platform has been developed as a plugin for Quantum GIS open source software, which offers many spatial

modelling programming capabilities. This paper describes the platform and proposes vector and raster based simulation results.

RÉSUMÉ. La pollution atmosphérique liée à l'usage agricole des produits phytosanitaires représente aujourd'hui un enjeu d'actualité pour la santé publique, pour l'agriculture durable et pour le contrôle de la qualité des écosystèmes. Un modèle de dispersion atmosphérique des pesticides a été développé à partir d'équations de la mécanique des fluides intégrées dans une programmation SIG pour fournir un outil de prédiction de la pollution de l'air. Ce travail concerne la modélisation de la dérive des pulvérisations lors des applications sur vigne, de l'échelle de la parcelle à celle du bassin versant. Notre objectif est de fournir une plateforme de simulation du transport à très faible coût de calcul en utilisant des techniques de réduction de l'espace. Cette méthode permet de fournir rapidement des prédictions de pollution géo-référencées qui peuvent par la suite servir de base pour une analyse de risque. Le couplage entre équations de mécanique des fluides et le SIG est tout d'abord décrit en insistant sur les modifications apportées au modèle mathématique pour l'intégration de données géographiques comme la topographie ou les variations d'échelle. En effet les variations de niveau du sol ont été intégrées dans le modèle à partir d'un modèle d'élévation numérique (DEM). L'utilisation du DEM permet aussi de remplacer les descriptions du nuage en coordonnées cartésiennes par des données raster et permet de travailler sur n'importe quelle zone. De plus l'intégration de la topographie dans la modélisation d'un nuage Gaussien spatialisé permet de travailler à plusieurs échelles. La plateforme a été développée sous la forme d'un plugin du logiciel libre Quantum GIS (QGIS) qui offre de nombreuses possibilités de programmation avancée. L'article présente les développements réalisés et les résultats des simulations vecteur et raster.

KEYWORDS: Atmospheric Dispersion, risk analysis, reduced-order modelling, Gaussian plume model, multi-scaled, digital elevation models, open source GIS development, Quantum GIS

MOTS-CLÉS : Dispersion Atmosphérique, Analyse de Risque, Modélisation d'ordre réduit, modèle Gaussien, multi-échelle, modèle d'élévation numérique, SIG libre, Quantum GIS

1. Introduction

Let us consider environmental phenomena presented by the atmospheric dispersion process. These are common in agricultural pesticide applications. The latter is part of our research interests, and this paper focuses on pesticide spray drift modelling over vineyards, using mathematical modelling and Geographical Information Systems (GIS). Our aim is to provide a platform dedicated to georeferenced atmospheric transport simulations at very low calculation cost, using reduced order modelling and open source GIS.

Atmospheric dispersion equations are based on parameters which are strongly affected by spatial and temporal variations [1]. These variations significantly affect the spray drift's behaviour and trajectory. The spatial dimension is thus essential in atmospheric dispersion modelling, but also represents the Geographical Information System's paradigm [2]. GIS have so become an adequate tool to analyze and visualize spatial based environmental models [3]. The coupling of the model with such technologies is presented here, regarding both the use of DEM and the role that GIS plays in the enhancement of the former model.

The optimization of the mathematical model regarding the spatial dimension first appears as necessary as we wish to couple a low-complexity model with the landscape representation provided by GIS. This work implies to establish links between the spray drift model and GIS algorithms, by selecting the most significant geospatial parameters that can improve the calculation. Topography effects and scale variations have been naturally chosen as one needed to get an optimized height dimension, in order to implement more reality in the drift phenomenon calculation. Then, a second side of the coupling consists in integrating the model within a GIS environment in the aim to manage and automate the model inputs and to promote its outputs using cartographic rendering.

In a previous work we have treated the problem of agricultural pesticide emission and dispersion, by coupling local (i.e. emission and near-field distribution) and global (i.e. transport over large distance) models [4, 6]. In this approach, the local model provides the inlet conditions for the levels above. The dependency between levels is a major asset to avoid the solution of partial differential equations using model reduction, as detailed in previous publications.[4, 5, 6, 7]

The goal of the present work is first to improve the existing long range transport model, and then to account for non uniform topographies to get more realistic simulations. We also want to be able to locally optimize the calculation accuracy according to scales variations, by using nested numerical zoom and modifying the wind flow field construction algorithm. Thus, two main aspects are presented in this paper. The optimisation of the dispersion model according to topography and scale changes is first presented using mathematical modelling. The coupling with GIS is then detailed in a second part, regarding the model integration and the main computational tasks.

2. Reduced-order modelling

2.1. Transport and non-symmetric geometry

We consider the situation of a source releasing a time dependent quantity $c_{inj}(t)$ in the atmosphere at a given location, and aim to develop a low-complexity model to represent the dispersion of this quantity. The primary factors influencing the dispersion of a neutral plume are advection by the wind and turbulent mixing. The simplest model of this process is to assume that the plume advects downwind and spreads out in the horizontal and vertical directions. Hence, the distribution of a passive scalar c , emitted from a given point and transported by a uniform plane flow field U along x coordinate, can be represented by:

$$c(x, y, z) = c_c(x)f(\sqrt{y^2 + z^2}, \delta(x)) \quad [1]$$

where

$$c_c(x) \sim \exp(-a(U)x)$$

and

$$f(\sqrt{y^2 + z^2}, \delta(x)) \sim \exp(-b(U, \delta(x))\sqrt{y^2 + z^2})$$

c_c is the behavior along the central axis of the distribution and $\delta(x)$ characterizes the thickness of the distribution at a given x coordinate. An analogy exists with plane or axisymmetric mixing layers and neutral plumes where δ is parabolic for a laminar jet and linear in turbulent cases [12, 8]. $a(\cdot)$ is a positive monotonic decreasing function and $b(\cdot, \cdot)$ is positive, monotonic increasing in U and decreasing in δ . In a uniform atmospheric flow field, this solution can be used for the transport of c^+ above.

This solution has been then generalized in a non symmetric metric defined by migration times calculation based on the flow field as explained in previous works [4, 5, 6, 7]. For ground variations modelling, the flow is locally rotated to remain parallel to the ground (see figure 1)

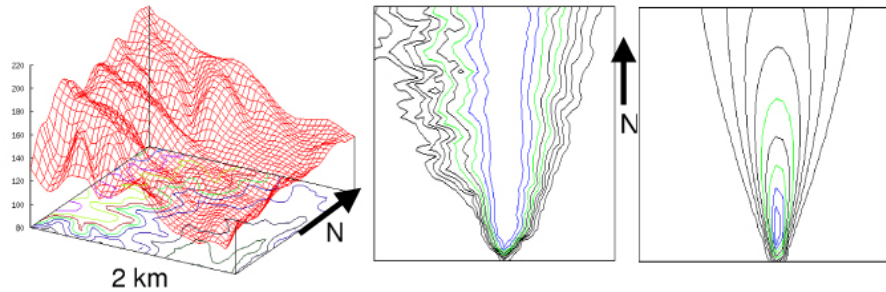


Figure 1. Left: A typical Digital Elevation Model (x and y coordinates range over 2 km). Atmospheric dispersion in a uniform north wind with (middle) and without (right) the DEM

2.1.1. Multi-level construction

In realistic configurations, simulation needs be carried out over several hundreds square kilometers domains. At the same time, we must be able to account for local topography variations with details provided every few meters. As wind measurements are most of the time available on very coarse grids, it is unrealistic and inefficient to perform the whole simulation with a metric topographic accuracy. Rather we would like to account large scale variations of topography on a coarse level simulation and include gradually the details of the ground variations near the main points of interest. To perform this task, one recursively applies the modelling described above on a cascade of embedded rectangular homothetic domains $\omega^i, i = 0, \dots$, with $\omega^0 = \Omega$ the full domain¹

No information is transferred at this time from fine to coarse. Indeed, we emphasize that the grids correspond to the locations where topography is available. As we mentioned, our approach is mesh free in the sense that no meshes is used for calculation. Only, evaluated information on wind and concentration are stored at these locations. The total wind field is expressed as:

$$\vec{U}_H = \sum_{i=0}^{n_{level}} \vec{u}^i \chi(\omega^i) \quad [2]$$

where $\vec{u}^0 = \vec{u}_H$ is calculated in equation for the coarser level and $\chi(\omega^i)$ is the characteristic function for the subdomain on which level i is defined. In other words, the correction is equal to zero outside ω^i . n_{level} is the total number of levels used. For $i > 1$, velocity restriction from level $i - 1$ to i is evaluated using the information from the observation point being the information at the four corners q_j of a rectangle:

$$\vec{u}^i = -\nabla \phi^i, \quad -\Delta \phi^i = 0, \quad \phi^i(q_j) = \phi^{i-1}(q_j), \quad j = 1, \dots, 4$$

Once again we can take advantage of the linearity of the operator, to use a similar decomposition for \vec{u}^i than for \vec{u}^0 where the observation quantities are becoming the values at the corners of the homothetic restriction:

$$\vec{u}^i(x) = \sum_{j=1}^4 \lambda_j(x) \vec{u}^{i-1}(q_j) \quad [3]$$

$$\text{Where } \sum_{j=1}^4 \lambda_j(x) = 1, \quad \text{and } \lambda_j(x_i) = \delta_{ij}, \quad i, j = 1, \dots, 4$$

If \vec{u}^{i-1} is divergence free, then this construction guarantees that

$$\int_{\partial \omega^i} \vec{u}^i \cdot \vec{n}^i dS = \int_{\partial \omega^i} \vec{u}^{i-1}|_{\partial \omega^i} \cdot \vec{n}^i dS = 0$$

1. For the sake of simplicity, and also because this is enough rich for environmental applications, we deliberately limit ourself to rectangular configurations.

Hence, the velocity restriction in ω^i remains divergence free and is compatible with the overall field. In the simulation presented here, three levels has been used to link $\Omega = \omega^0 \sim 10km^2$ to the $\omega^2 \sim 10m^2$.

Once the velocity restriction is defined, the concentration restriction is calculated as follow:

$$c^i = \sum_{j=1}^4 \lambda_j(x) c^{i-1}(q_j) \quad [4]$$

This construction guarantees that the total mass in ω^i fits the entering quantity ²:

$$\int_{\omega^i} c^i dV = \int_{\partial\omega^i} c^i \left(\frac{\vec{u}^i}{\|\vec{u}^i\|} \cdot \vec{n}^i \right) dS$$

In practice, we use the same sampling for each level, typically a 20×20 grid which means topography needs to be defined every 500 meters at coarse level and every 50 cm at the finest level. This is interesting as it permits to locally provide a more accurate Digital Elevation Model.

2.1.2. Integral data

Once the species distribution $c(x, y, z)$ is found and that the total injected quantity in time interval $[0, T]$ is known, one can assumes:

$$K = \int_0^T c_{inj}(t) dt$$

Various quantities can be computed. For instance, we can have an estimation of the amount of species which has reached the ground using:

$$C_g(x, y) = \int_{z \leq z_0} c(x, y, z) dz$$

or estimate the quantity still in the atmosphere beyond a distance R_0 from the source, using:

$$C_a = K - \int_{R \geq R_0} C_g(x, y) dV$$

$R = \sqrt{x^2 + y^2}$ corresponds to the radius from source.

2.2. Multilevel correction for ground variations

2.2.1. Multi-level correction

At this point we would like to account for the topography or ground variations ($(x, y) \rightarrow \psi(x, y)$) in the prediction model above. These are available from Digital Elevation Models (DEM) [26],[25]. Despite this plays an important role in the

2. The four points trapezoidal rule is exact for numerical integration of bilinear functions $\int_{\omega} f(x, y) dx dy = \frac{1}{4} \sum_{j=1}^4 f(q_j)$.

dispersion process, it is obviously hopeless to launch direct simulations using a Computational Fluid Dynamic (CFD) model, based on a detailed ground description . We should mention that ground variations effects are implicitly present in observation data for wind. However, as we said, wind observations are quite incomplete. In particular, wind measurements are available every few kilometers while topographic data are available on a metric basis. At each level i of the construction (see figure 2) we introduce a correction \vec{u}_t^i to the restriction

$$\vec{U}_H = \sum_{i=0}^{n_{level}} (\vec{u}^i + \vec{u}_t^i) \chi(\omega^i) \quad [5]$$

Various local modelling can be considered for \vec{u}_t^i going from simple algebraic expres-

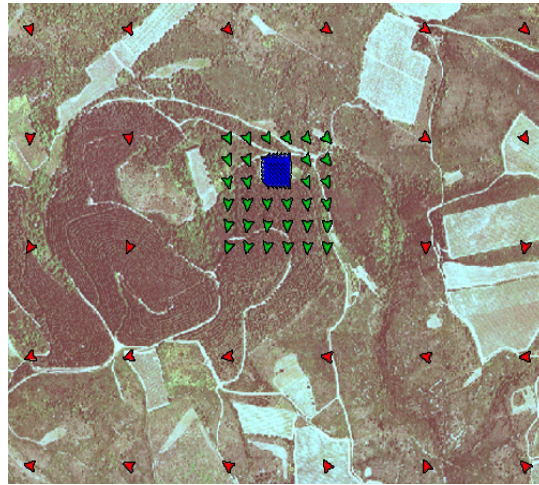


Figure 2. Example of three-level construction of a flow field, generated by the model and loaded into GIS as a vectorial layer.

sions to more sophisticated local CFD models. We propose the following correction³

$$\vec{u}_t^i = -\frac{1}{\rho} \text{sgn}(U_t) \nabla p^i, \quad p^i = p_r^{i-1} U_t^2 \quad [6]$$

where

$$U_t = \frac{\vec{u}^{i-1}}{\|\vec{u}^{i-1}\|} \cdot \vec{n}_t^i \quad \text{and} \quad p_r^{i-1} = \frac{1}{2} \rho (\vec{u}^{i-1} \cdot \vec{n}_t^i)^2$$

3. This is the Bernoulli-Newton formula widely used in aeronautics and reproducing well the pressure distribution over a cylinder for a potential flow.

ρ is the density of the fluid. p_r is a local pressure reference based on averaged entering velocity into subdomain i :

$$(\vec{u}^{i-1} \cdot \vec{n}^i)_- = \frac{1}{n_-} \sum_{j=0}^4 \min(0, \vec{u}^{i-1}(q_j) \cdot \vec{n}_j^i)$$

$1 \leq n_- < 4$ being the number of entering flow corners. The normal to the ground evaluated from the digital terrain model restriction at level i is denoted by \vec{n}_t^i . This is different from the normal \vec{n}^i to subdomain i . In absence of ground variations the two normals are orthogonal (see figure 3).

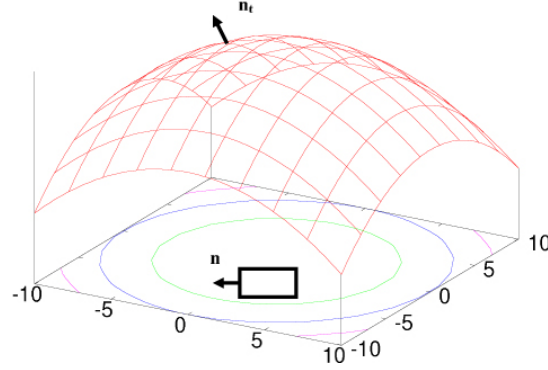


Figure 3. Sketch of topography variation and normals definitions

In case the topography is not constant, we have

$$\vec{u}^{i-1} \cdot \vec{n}_t^{i-1} = 0, \text{ but } \vec{u}^{i-1} \cdot \vec{n}_t^i \neq 0$$

This multi-level correction improves the predictive capacity of the model introducing a dependency between ground variations and migration time. However, this is not sufficient to correctly account for ground variations in dispersion. For instance, it is indeed clear that, even in a uniform flow, cross diffusion is not symmetric on a slopy ground when dispersion is performed parallel to the iso-level contours (see figure (see figure 4)).

We also need to correct the functions a and b appearing in the dispersion modelling. As we have assumed the construction is only coarse to fine without feedback from fine to coarse levels, we assume the correction conservative in the sense that the incoming mass into subdomain i :

$$\begin{aligned} K^i &= \left(c^{i-1} \frac{\vec{u}^{i-1}}{\|\vec{u}^{i-1}\|} \cdot \vec{n}^i \right)_- \\ &= \frac{1}{n_-} \sum_{j=0}^4 \min \left(0, c^{i-1}(q_j) \frac{\vec{u}^{i-1}(q_j)}{\|\vec{u}^{i-1}(q_j)\|} \cdot \vec{n}_j^i \right) \end{aligned}$$

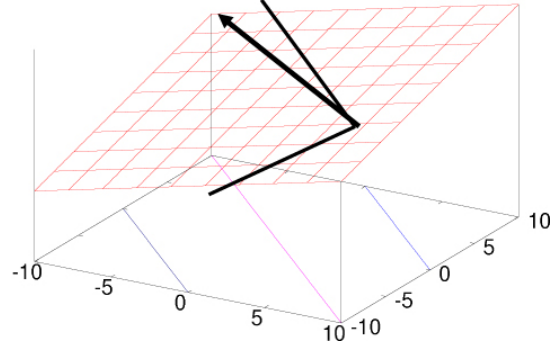


Figure 4. Sketch of topography variation and non symmetry in cross-definition for a constant velocity field

defines the integral expression with or without topography changes:

$$K^i = \int_{\omega^i} c^i dV = \int_{\omega^i} c_t^i dV$$

where c_t is the modified expression for the concentration to account for topography changes and \vec{n}_j^i is the normal to face $j = 1, \dots, 4$ of subdomain i . This implies a constraint on the modified expressions of a and b (e.g. correction on b can be deduced from a) through our analytical dispersion model.

$$K^i = \int_{\omega^i} c_t^i(a, b) dV \quad [7]$$

The correction in a is a scaling by a positive monotonic decreasing function worthing one in absence of topography changes. For instance, one can assume:

$$a_t^i = a^i \frac{\|\vec{u}^i + \vec{u}_t^i\|}{\|\vec{u}^i\|}$$

Hence, in case a change in topography increases the local velocity the dispersion goes further downstream with less cross-diffusion due to decreasing b through constraint.

3. GIS based coupling

3.1. Linking Dispersion model and GIS

It should first be reminded that we want to couple the above physical model which involves unsteadiness and uncertainties, with GIS that are tending to provide an accurate numerical copy of the study area's surface. Thus, GIS can be used to apply the model in a richer georeferenced numerical environment. GIS capabilities regarding DEM generation and exploitation are significantly improving the former dispersion

equations, as they allow the model to be run on any local topography [26]. Furthermore, GIS permits to map directly the drift process and to get standard atmospheric concentrations at given geographical coordinates. Then it becomes rather easy to make the pesticide cloud interact with other relevant geodata, and so to proceed to advanced risk analysis [32] regarding for example bystanders exposure, agricultural plots or water courses contamination after treatments. Although GIS allows to gain some more precision regarding topographic impact on calculations and to georeference the model outputs, we should keep in mind that the main objective of the reduced order modelling approach is to provide mean tendencies of the spray drift with very low calculation cost, and that potential errors are duplicated into the GIS. In addition to this, automated geoprocessing tasks that are carried, like DEM generation or point-based data interpolation can also add some more spatial incoherence and introduce a new level of uncertainties. As those limits regarding precision and application on real situation have been raised, it is now interesting to explain more precisely how the model and GIS communicate, and how we can get the best of geospatial techniques to improve the model's efficiency.

3.1.1. *Loose coupling method*

Several ways to couple GIS and environmental models are known in literature, mainly "tight" or "loose" coupling and more recently "integrating" systems [20, 21]. Each technique presents assets and limitations, and is more or less adapted depending on the complexity of the model. In our case, the loose coupling has been chosen for several reasons that have to be explained. As the latest describes an approach where interfaces are developed with minimal assumptions between the sending/receiving parties, therefore the risk that a change in one application will force a change in another application is reduced [22]. Loose coupling has also multiple assets regarding development costs, as we want to couple the model with existing GIS, and not coding a entire GIS software able to implement natively the dispersion model, as the integrated approach would suggest. As more and more GIS programs are being made available by open-source communities, we opted for Quantum GIS (QGIS) software to achieve the coupling, as it is one of the most highly capable open-source tool which offers advanced programming possibilities [27]. Indeed, QGIS is based on a robust $C++$ API that presents plenty of spatial algorithms and native GIS functions. Those have been made accessible through Python bindings, which allow a simpler programming environment for developing specific QGIS plugins that directly interact with the core source code [28]. We opted for this technical solution to propose a friendly-user atmospheric pesticide spray drift plugin. It is dedicated to agricultural atmospheric pollution prediction, and has been designed to be fast and extensible, mixing reduced-order modelling and GIS development.

3.1.2. *GIS as input data provider*

The first roles of GIS deals with the automatic DEM extraction, needed by the model to compute the effects of ground variations on the windfield and so on the pesticide cloud movements. As the multi-levelled approach has been conceptualized to

gain in topographic accuracy, one has to work with several DEM resolutions and must be able to extract pixel values from any loaded DEM in the GIS. Using the Python bindings, this can simply be done with some common GDAL (Geospatial Data Abstraction Library)⁴ commands. In our case we use two successive *gdal translate* commands [30], as described below:

```
gdal_translate -ot Float32 -projwin "str(xmin) + str(ymax) +  
    str(xmax) + str(ymin)+" input_dem.tif output_dem.tif
```

This first command is done to clip the loaded DEM according to the user defined extent in which the calculation must be launched.

```
gdal_translate -of AAIGrid clip.tif clip.asc
```

And this one to extract the elevation value of each pixel of the extent to an ESRI grid file [31]. The obtained grid is then converted into x,y,z triplets [34] needed by the model as topography inputs, using the *grd2xyz* python class⁵. These successive commands permit to get the topographic input data for the dispersion model, overriding the user's DEM resolution and spatial projection as the Fortran program is then able to convert cartesian metric into the same values it reads in input.

3.2. Spatialisation of the model

Once those input parameters are being made available for QGIS, we must use them to provide a georeferenced environment for the model's output data. This step deals both with some basic file format conversion, the multi-leveled equation implementation and some advanced geodata processing. The georeferencing technique is first presented, and then we show how the GIS deals with the multi-scaled dispersion model. Some cartographic ramblings are finally presented, regarding the best way to map pesticide atmospheric drift.

3.2.1. Georeferencing the model's topographic input data

The mathematical model works on a cartesian metric basis, which is not readable as is by QGIS. As we want the plugin to be able to read any resolution in any geographic projection, the spatial properties of the image DEM have to be read and understood by the model. This is done by sending the resulting file of the *gdal translate* commands to the Fortran program, which one reads the given tabular x,y,z file by accessing the standard Comma Separated Values (CSV) format [30]. The generated DEM is sent to Fortran using simple Fortran *open*, *do* and *read* commands: Each

4. The GDAL/OGR open source library was developed by Franck Warmerdam, independent developer from Egganville (CA) and president of OSGeo since 2006.

5. This code is inspired from one of David Finlayson from the United States Geological Survey, Santa Cruz (USA).

triplets (i.e each line of the former raster matrix) is then understood by Fortran and provides the elevation data on which the calculation have to be computed, for every point of the domain.

3.2.2. Introducing the multi-leveled algorithm

The multi-leveled correction for ground variations let the user choose the number of levels wanted (i.e $nlevels$ in equation (10)), as well as their spatial extent (see figure 2). This permits to define the local area where the DEM resolution must be finer in order to compute ground variations more precisely. This "micro-scale" area can be defined for example just around the considered source plot or any other area that presents particular topography or significant obstacle (like local depression, small hill or other interesting rock-formings) to the spray drift. This is done in QGIS using an adaptation of the *Region Tool*⁶ algorithm [33] applied in a recursive way:

```
def doneRectangle(self):
    level = self iface.getMapCanvas().setMapTool(self.
        saveTool)
    self.updateBounds(self.r.bb)
```

This first function permits to draw and save a rectangle on QGIS map view (map canvas) that defines the new extent.

```
def updateBounds(self, bb):
    self.xmindomain.setText(str(bb.xMin()))
    self.ymindomain.setText(str(bb.yMin()))
    self.xmaxdomain.setText(str(bb.xMax()))
    self.ymaxdomain.setText(str(bb.yMax()))
    newLevel = bb.xMin(), bb.yMin(), bb.xMax(), bb.yMax()
```

Then, the previous code allows to update the four corners of the extent and so to determine a new level for calculation. This way *Region Tool* can be used as many times as wanted, in order to set up the right number of levels for the calculation.

3.2.3. Cartography of pesticide clouds

The last step of the plugin development concerns the conversion of CSV outputs into standard GIS formats, but also the way one can enhance the cartographic rendering of the pesticide cloud. Using the QGIS API once again, we can first easily generate the model output results as ESRI shapefile (.shp) or any other OGR supported GIS vector format. This is done using the QGIS *QgsVectorFileWriter* class as presented below:

```
uri="plume.csv?delimiter=%s&xField=%s&yField=%s"%( ";" , "
    longitude" , "latitude" )
```

6. This code is inspired from one of Barry Stephen Rowlingson from the Mathematics and Statistics department of Lancaster University (UK).

```
v=QgsVectorLayer(uri,"vectorial_plume")
QgsVectorFileWriter.writeAsShapefile(v,"vectorial-plume.shp"
    ')
```

Where plume.csv is the input CSV file that include longitude, latitude and atmospheric concentrations fields, and vectorial-plume.shp is the created point shapefile. Once this done, one can instantaneously apply some styling options to the created layer, in order to emphasize the concentrations values. This can be done using the QGIS *QgsContinuousColorRenderer* class, by allotting a symbol type to the geometries and a couple of minimum and maximum colors for the continuous color rendering (see figure 5).

```
r=QgsContinuousColorRenderer(v.vectorType())
r.smin=QgsSymbol(v.vectorType(),"0","","")
r.smax=QgsSymbol(v.vectorType(),"1","","")
r.smin.setPen(QPen(Qt.green,1.0))
r.smax.setPen(QPen(Qt.red,1.0))
```

Thus, the resulted vectorial pesticide cloud is readable by any standard GIS program, and can be used in a simpler way for spatial analysis and atmospheric pollution prediction.

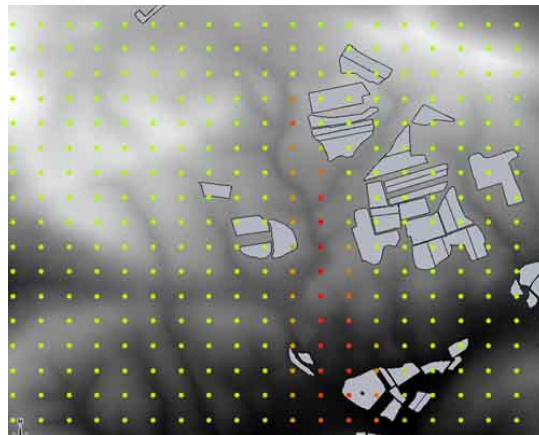


Figure 5. Example of vectorial pesticide cloud generated as ESRI Shapefile (.shp) with applied graduated color on the concentration field.

Another point of interest for mapping pesticide clouds is the raster generation, as the spray drift is a diffuse phenomenon and that a surfacic representation is much more readable than points in this case. The raster creation can significantly improve the cartographic message. In order to interpolate point-based values, one opted for the inverse distance algorithm, assumuming that the nearer a point to be interpolated is located to a point with known value, the more similar is the value of the point to be interpolated to the known value in close distance. This can be done using the *gdal*

grid interpolation capabilities, using the GDAL virtual format (i.e VRT driver) [30] and playing on the power and smoothing values:

```
gdal_grid -a invdist:power=1.0:smoothing=50.0 -tse"+str(xmin
)+str(xmax)+"-tse"+str(ymin)+str(ymax)+"
-of GTiff -ot Float64 -l driftx driftx.vrt output.tif".
readlines()
```

Where *-tse* is the spatial extent in which to interpolate (i.e the user defined extent via the Region Tool class), *-of* is the desired output format and *-ot* the raster type. As the point-based values are interpolated over the whole domain, one has to apply a vectorial mask, in order to account only for points with values and so to kill the raster nodata. This can be done using the clipping functions of GDAL, using a *gdal -clip* command line. Finally and as for the vector outputs, one can apply coloring schemes and transparency values, using the QGIS *QgsRasterLayer* optionnal arguments (see figure 6), as suggested below:

```
r=QgsRasterLayer(fileName, baseName)
r.setDrawingStyle(QgsRasterLayer.SINGLE_BAND_PSEUDO_COLOR)
r.setColorShadingAlgorithm(QgsRasterLayer.PSEUDO_COLOR)
r.setTransparency(90)
```

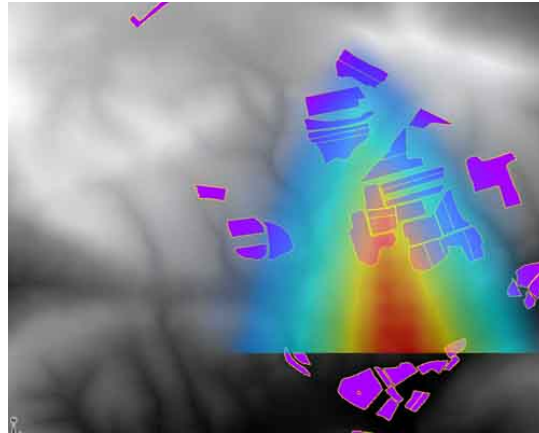


Figure 6. Example of interpolated and masked raster pesticide cloud.

4. CONCLUSION AND PERSPECTIVES

A low-complexity model for the prediction of passive scalar dispersion in atmospheric flows has been presented and coupled with open source GIS. The solution search space has been reduced using a priori physical information and a non symmetric metric based on migration times has been used to generalize injection and plume similitude solutions in the context of variable flow fields.

The pesticide spray drift model has been applied on realistic topographic input data through coupling the inputs reading method with digital terrain models. Some of the GIS capabilities regarding spatial data storage and management have thus been exploited in order to fit better to the vineyards landscape reality and so to tend to a true to life calculation.

Furthermore, the multi-level algorithm and its correction for ground variations provides more accuracy. Current work now deals with the optimisation of the reading and the interpretation of the topographic data, but also with the integration and the use of several DEM into a single domain and in its implementation in the Python plugin. This is one more link between fluid mechanics equations and GIS algorithms to be established. In order to fully validate the topography effect, one will also have to realize simulations over longer time-series and different kind of slopes and micro-relief, in order to compare the resulting values with real atmospheric concentration values. To achieve the terrain validation, a agricultural watershed will be monitored with air sampling devices that have to be positioned according to the major wind flows. Comparison between numerical results and chemical air analysis are planned for the future.

Finally, a Quantum GIS python plugin for atmospheric pollution prediction has been presented and detailed by illustrating the coupling concepts and explaining some of the functional code snippets. One of the major asset of the reduced-order modelling approach is to simplify the programming aspects of the coupling, and the same logic has been used regarding the open source GIS development. The result is that both dispersion model and GIS can communicate each other but stay independent. Although the plugin is already an usable and friendly-user tool for pollution prediction, some more improvements have to be developed in order to provide optimised wind flow and pesticide clouds calculation and also additional automated GIS functionalities.

5. References

- M. Markiewicz -2006, *Modelling of air pollution dispersion*, Technical Report, **2511**, 2006.
- Dragosits,U. and Place,C.J. and Smith,R.I. -1996, *The Potential of GIS and Coupled GIS/Conventional Systems to Model Acid Deposition of Sulphur Dioxide*, Third International Conference/Workshop on Integrating GIS and Environmental Modeling, **2511**, 1996.
- Karimi,H. and Houston,B. -1997, *Evaluating strategies for integrating environmental models with GIS: current trends and future needs*, Computers, Environment and Urban Systems, Elsevier, vol.20 **2511**, 1997.
- Brun J-M. *Modélisation à complexité réduite de la dérive*. Thesis University of Montpellier. 2006.
- Brun J-M. and Mohammadi B. -2007, *Similitude généralisée et modélisation géométrique à complexité réduite*, Comptes Rendus Académie des Sciences, **2511**, 2006.
- B. Mohammadi, J.M. Brun, O. Pironneau *Reduced order modelling of dispersion* 2006. Numerical Analysis and Scientific Computing with pde and their challenging applications, Springer.

- N.Bozon, B. Mohammadi and C.Sinfort *Similitude and non symmetric geometry for dispersion modelling* Special issue STIC and Environnement'07, e-sta vol.5,2008
- Simpson J. *Gravity currents in the environment and laboratory* 1997. Cambridge University Press, 2nd edition.
- Mohammadi B. and Pironneau O. *Applied shape optimization for fluids*. 2001. Oxford Univ. Press.
- Ciarlet Ph. *The finite element method for elliptic problems*. 1978. North-Holland.
- Veroy K. and Patera A. *Certified real-time solution of the parametrized steady incompressible Navier-Stokes equations: Rigorous reduced-basis a posteriori error bounds* Int. J. Numer. Meth. Fluids. 2005. **47/2**:773-788.
- Cousteix J. *Turbulence et couche limite*. 1989. Cepadues publishers.
- Alauzet F. George P-L. Frey P. Mohammadi B. *Transient fixed point based unstructured mesh adaptation*. Int. J. Numer. Meth. Fluids. 2002. **43/6**:729-745.
- Hecht F. and Mohammadi B. *Mesh adaptation by metric control for multi-scale phenomena and turbulence*. AIAA paper 1997-0859.
- Borouchaki H. George P-L. Mohammadi B. *Delaunay mesh generation governed by metric specifications*. 1997. Finite Element in Analysis and Design. **2**:85-109.
- Krige, D.G. *A statistical approach to some mine valuations and allied problems at the Witwatersrand*. 1951. Master's thesis of the University of Witwatersran.
- Chiles, J.-P. and P. Delfiner *Geostatistics, Modeling Spatial uncertainty*. 1999. Wiley Series in Probability and statistics.
- Nektarios, P. A., Lee, P. C., Steenhuis, T. S., Timmons, M. B., Haith, D. A. *Modeling pesticide volatilization from turf*. 2004. Acta Horticulturae, (No. 661) 433-440.
- Mohammadi B. & Pironneau O. *Analysis of the k-epsilon turbulence model*. 1994. Wiley.
- Karimi H. & Houston B. *Evaluating strategies for integrating environmental models with GIS: current trends and future needs*. 1997. Computers, Environment and Urban Systems.
- Huang B. & Jiang B. *AVTOP: a full integration of TOPMODEL into GIS*. 2001. Environmental Modelling and Software.
- Corwin D. & Wagenet R. *Applications of GIS to the Modeling of NonPoint Source in the Vadose Zone: A Conference Overview*. 1996. Journal of Environment Quality.
- Santilli S. & Leslie M. & Hodgson C. & Ramsey P. *PostGIS manual*. 1996. PostGIS Refractions website (<http://postgis.refractions.net/docs>).
- Mohammadi B. & Puigt G. *Wall functions in computational fluid dynamics*. 2006. Computers & Fluids, **40-3**:2101-2124.
- ArcGIS *Geographic Information System* 2006. <http://www.esri.com/software/arcgis>
- Maune D., Kopp S., Crawford C., and Zervas C. *Digital Elevation Model Technologies and Applications: The DEM Users Manual 2nd edition (introduction)*. 2007. American Society for Photogrammetry and Remote Sensing
- Sherman G. & Sutton T. & Blazek R. & Mitchell T. *Quantum GIS Software User Guide*. 2007. Quantum GIS Documentation website (<http://gisalaska.com/qgis/doc>).
- Sherman G. & Sutton T. & Blazek R. & Mitchell T. *Quantum GIS API Documentation*. 2007. Quantum GIS API Doc (<http://doc.qgis.org/>).

- Page C.G *Professional Programmer's Guide to Fortran 77*. 2005. University of Leicester website (<http://www.star.le.ac.uk/cgp/prof77.html>).
- Warmerdam F. *GDAL/OGR API Documentation*. 2005-2008. GDAL/OGR website (<http://www.gdal.org/>).
- Tomlinson R. *Thinking about GIS: Geographic Information System Planning for Managers*. 2007. ESRI, Inc.
- Halls P. *Spatial Information and the Environment*. 2001. CRC Press.
- Rowlingson B.S *Region Tool Algorithm*. 2007. Barry Stephen Rowlingson personal website (<http://www.maths.lancs.ac.uk/rowlings/Software/regionTool>).
- Finlayson D. *grd2xyz - Grid to x,y,z converter python script*. 2007. David Finlayson personal website (<http://david.p.finlayson.googlepages.com/gisscripts>).